Reaction of Ferrate(VI) with ABTS and Self-decay of Ferrate(VI): Kinetics and Mechanisms.

ARTICLE *in* ENVIRONMENTAL SCIENCE & TECHNOLOGY · APRIL 2014

Impact Factor: 5.33 · DOI: 10.1021/es500804g · Source: PubMed

3 AUTHORS, INCLUDING:

Yunho Lee
Gwangju Institute of Science and Technology
33 PUBLICATIONS **1,137** CITATIONS
SEE PROFILE

Reinhard Kissner
ETH Zurich
69 PUBLICATIONS **2,123** CITATIONS
SEE PROFILE

Environmental Science & Technology

Article

pubs.acs.org/est

Reaction of Ferrate(VI) with ABTS and Self-Decay of Ferrate(VI): Kinetics and Mechanisms

Yunho Lee,[†,‡] Reinhard Kissner,[§] and Urs von Gunten[†,∥,⊥,*]

[†]Eawag, Swiss Federal Institute of Aquatic Science and Technology, Ueberlandstrasse 133, CH-8600 Duebendorf, Switzerland

[‡]Department of Environmental Science and Engineering, Gwangju Institute of Science and Technology (GIST), Gwangju 500-712, Republic of Korea

[§]Institute of Inorganic Chemistry, Department of Chemistry and Applied Biosciences, ETH Zurich, CH-8092 Zurich, Switzerland

[∥]Institute of Biogeochemistry and Pollutant Dynamics, ETH Zurich, CH-8092 Zurich, Switzerland

[⊥]School of Architecture, Civil and Environmental Engineering (ENAC), Ecole Polytechnique Fédérale de Lausanne (EPFL), CH-1015, Lausanne, Switzerland

Supporting Information

ABSTRACT: Reactions of ferrate(VI) during water treatment generate perferryl(V) or ferryl(IV) as primary intermediates. To better understand the fate of perferryl(V) or ferryl(IV) during ferrate(VI) oxidation, this study investigates the kinetics, products, and mechanisms for the reaction of ferrate(VI) with 2,2′-azino-bis(3-ethylbenzothiazoline-6-sulfonate) (ABTS) and self-decay of ferrate(VI) in phosphate-buffered solutions. The oxidation of ABTS by ferrate(VI) via a one-electron transfer process produces $ABTS^{\bullet+}$ and perferryl(V) ($k = 1.2 \times 10^6\ M^{-1}\ s^{-1}$ at pH 7). The perferryl(V) mainly self-decays into H_2O_2 and Fe(III) in acidic solution while with increasing pH the reaction of perferryl(V) with H_2O_2 can compete with the perferryl(V) self-decay and produces Fe(III) and O_2 as final products. The ferrate(VI) self-decay generates ferryl(IV) and H_2O_2 via a two-electron transfer with the initial step being rate-limiting ($k = 26\ M^{-1}\ s^{-1}$ at pH 7). Ferryl(IV) reacts with H_2O_2 generating Fe(II) and O_2 and Fe(II) is oxidized by ferrate(VI) producing Fe(III) and perferryl(V) ($k = \sim 10^7\ M^{-1}\ s^{-1}$). Due to these facile transformations of reactive ferrate(VI), perferryl(V), and ferryl(IV) to the much less reactive Fe(III), H_2O_2, or O_2, the observed oxidation capacity of ferrate(VI) is typically much lower than expected from theoretical considerations (i.e., three or four electron equivalents per ferrate(VI)). This should be considered for optimizing water treatment processes using ferrate(VI).

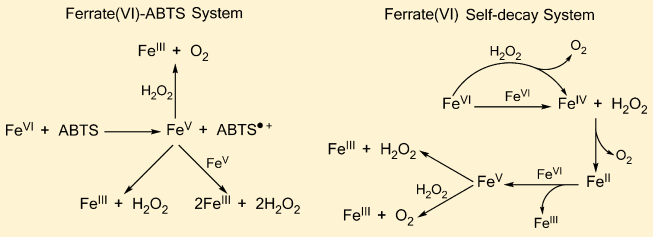

INTRODUCTION

In recent years, ferrate(VI) has received increased attention as a potential water treatment chemical due to its dual functions as an oxidant and a subsequent coagulant as ferric hydroxides.[1−18] Due to this interest in ferrate(VI) chemistry, kinetics, and mechanisms of ferrate(VI) reactions in water were studied as a basis for its successful application to water treatment. Currently, there are ∼150 second-order rate constants (k) available in literature for ferrate(VI) reactions with various (in)organic compounds.[19,20] Most rate constants known in literature are limited to basic aqueous solution (e.g., pH > 7) and thus further kinetic information is required covering the rest of the pH range, because ferrate(VI) exists in four different protonation states in aqueous solution (eqs 1−3)[21,22] and its reactivity varies significantly depending on its speciation.[19,20]

$$H_3Fe^{VI}O_4^{+} \rightleftharpoons H_2Fe^{VI}O_4 + H^+ \quad pK_1 = 1.5^{21} \tag{1}$$

$$H_2Fe^{VI}O_4 \rightleftharpoons HFe^{VI}O_4^{-} + H^+ \quad pK_2 = 3.5^{22} \tag{2}$$

$$HFe^{VI}O_4^{-} \rightleftharpoons Fe^{VI}O_4^{2-} + H^+ \quad pK_3 = 7.2^{22} \tag{3}$$

Ferrate(VI) has been proposed to react with (in)organic compounds via one-electron or two-electron transfer mechanisms. For examples, the reaction of ferrate(VI) with phenol produces perferryl(V) and phenoxyl radicals as primary products via a one-electron transfer.[23] In contrast, a two-electron transfer mechanism has been proposed for the reaction with hydroxylamine via two-consecutive hydrogen abstractions[24] and for sulfite via oxygen transfer,[25,26] where ferryl(IV) is produced as a primary reaction intermediate. It was also proposed that cyanides, iodide, and the superoxide radical react via a one-electron transfer mechanism while arsenite, hydrogen peroxide, hydroxylamine, selenite, and sulfite react via a two-electron transfer mechanism with ferrate(VI).[27] These assumptions were based on a linear correlation between the second-order rate constants and one/two reduction potentials and observed reaction stoichiometries and products.

Received: February 16, 2014
Revised: March 28, 2014
Accepted: April 3, 2014
Published: April 3, 2014

   dx.doi.org/10.1021/es500804g | Environ. Sci. Technol. 2014, 48, 5154−5162

Perferryl(V) species are three to six orders of magnitude more reactive than ferrate(VI) for their reactions with various compounds.[19,20] In contrast, limited information exists for the reaction kinetics of ferryl(IV) species in neutral or basic solutions albeit the reaction kinetics and mechanisms have been studied in acidic solutions.[28−32] One study showed that ferryl(IV) and perferryl(V) reacted two- and four-orders of magnitude faster than ferrate(VI) with cyanide in basic solutions.[33] Based on this, perferryl(V) and ferryl(IV) species may contribute to an enhanced oxidation of compounds that are less reactive with ferrate(VI). However, the fate of perferryl(V) and ferryl(IV) during ferrate(VI) oxidation processes is currently poorly understood. Perferryl(V) and ferryl(IV) species are known to undergo "self-decay" and transform into iron(III), oxygen or hydrogen peroxide (H_2O_2) as products.[34−36] However, only few ferrate(VI) reactions have been fully characterized and understood with respect to the formation and fate of perferryl(V) and ferryl(IV) species. To better quantify the overall reaction mechanisms, the competiton of perferryl(V)/ferryl(IV) species for reactions with target compounds and their self-decay has to be understood.

The reaction of ferrate(VI) with 2,2′-azino-bis(3-ethylbenzothiazoline-6-sulfonate) (ABTS = $HABTS^-$/$ABTS^{2-}$) has been used as a method to determine aqeuous ferrate(VI) concentrations based on the formation of a green radical cation ($ABTS^{\bullet+}$) [$HABTS^+$/ABTS/$ABTS^{\bullet+}$ are used in this study to express the conceptual charge on the nitrogen moiety of ABTS. The formal charge of $HABTS^+$/ABTS/$ABTS^{\bullet+}$ are '−1/−2/−2', respectively due to the presence of two sulfonate groups] that can be measured spectrophotometrically at 415 nm.[37] The formation of $ABTS^{\bullet+}$ as one-electron oxidation product indicates that perferryl(V) is primarily produced from the reduction of ferrate(VI). The observed 1:1 stoichiometry (not 1:3) of the ferrate(VI)-ABTS reaction was explained by an oxidation of ABTS by perferryl(V) to an unknown colorless product.[37] However, a potential perferryl(V) self-decay was not considered previously. Detailed kinetic and mechanistic information for the reaction of ferrate(VI) with ABTS is expected to provide useful information for a better understanding of the fate of the perferryl(V) species during ferrate(VI) oxidation reactions.

Ferrate(VI) is unstable in aquous solution at pH below 9 and has been known to decompose to Fe(III) and oxygen (O_2) as final products.[21,25,38,39] The reaction order for the ferrate(VI) self-decay has been disputed in literature. Mixed first- and second-order decay kinetics with respect to the ferrate(VI) concentration have been reported in some studies[25,38] while second-order decay kinetics have been observed in other studies.[21,39] The mechanisms for ferrate(VI) self-decay have been recently proposed in acidic pH solutions[39] which involve the formation of a diferrate(VI) species via dimerization of a monomeric ferrate(VI) and subsequent intramolecular oxo-coupling leading to a production of O_2 and a diferryl(IV) species. Nevertheless, the ferrate(VI) self-decay mechanism at near-neutral pH, which might differ significantly due to the involvement of less protonated ferrate(VI) species (e.g., $H_3Fe^{VI}O_4^+$ at pH 1 vs $HFe^{VI}O_4^-$ at pH 7), is still poorly understood.

To build concrete models for aqueous ferrate(VI) reactions, this study investigates two important aqueous ferrate(VI) reactions, that is, the reaction of ferrate(VI) with ABTS and self-decay of ferrate(VI), which are not only relevant for ferrate(VI) applications to water treatment but also provide basic information on the fate of perferryl(V) and ferryl(IV) species during ferrate(VI) oxidation. Taking the reaction of ferrate(VI) with ABTS as a model system for the initial one-electron transfer generating perferryl(V), the mechanisms of ferrate(VI) self-decay were investigated by measuring the yield of H_2O_2 as a common product of both reactions. Kinetic studies were performed for both reactions in phosphate buffered solutions in the pH range from 1 to 12. Products and stoichiometries were investigated in the pH range 2.9−8.8 for the reaction of ferrate(VI) with ABTS and mainly at pH 7 for the ferrate(VI) self-decay. A kinetic model was formulated using the proposed elementary reactions and the corresponding reaction rate constants and then validated by comparing experimental and simulated concentration profiles of reactants and products.

EXPERIMENTAL SECTION

Standards and Reagents. All chemicals and solvents (95% purity or higher) were used as received from various commercial suppliers. Description on preparation of solutions and quantification of ferrate(VI), Fe(III), Fe(II), and H_2O_2 are provided in the Supporting Information (SI), SI Text-1.

Reaction Kinetics. Kinetic studies of ferrate(VI) reactions were performed in the pH range 1−12 at 24 ± 1 °C. For all pH conditions, phosphate was used as a buffer as well as a complexing agent for Fe(III). Details of the buffer conditions are provided in SI Text-2.

Kinetics for the reaction of ferrate(VI) with ABTS were investigated using an Applied Photophysics SX−17MV stopped−flow spectrophotometer. Second-order rate constants for the reaction of ferrate(VI) with ABTS were determined under pseudo-first-order conditions for ferrate(VI) in excess of ABTS in the pH range 1.4−9.8. Absorbance increases at 415 nm were monitored, which are equivalent to the formation of $ABTS^{\bullet+}$ and ferrate(VI) decrease.

Kinetics of ferrate(VI) self-decay were investigated in the pH range 1.0−8.2 either by using an Applied Photophysics SX-17MV stopped-flow spectrophotometer (t = 10 ms −10 s) or a Hi-Tech SFA 20 rapid mixing unit connected to a HP 8452 diode array UV−vis spectrophotometer (t > 1 s) by measuring the absorbance at 510 nm for ferrate(VI). Ferrate(VI) self-decay kinetics were also studied in a conventional batch reactor by measuring the ferrate(VI) decrease using the ABTS colorimetric method (t > 20 s).[37]

Second-order rate constants for the reaction of ferrate(VI) with H_2O_2 were determined by measuring ferrate(VI) decreases with the ABTS method[37] in the pH range of 6−12. Kinetics for the reaction of ferrate(VI) with Fe(II) were investigated using an Applied Photophysics SX-17MV stopped-flow spectrophotometer by measuring absorbance decreases at 510 nm for ferrate(VI) at pH 5.

Reaction Products. The consumption of ABTS and the formation of $ABTS^{\bullet+}$ and H_2O_2 were determined after the reaction of ABTS (80 μM) with ferrate(VI) (2−24 μM) in the pH range of 2.9−8.8. ABTS and $ABTS^{\bullet+}$ were quantified by measuring the absorbance at 340 and 415 nm and using the molar absorption coefficients of ABTS and $ABTS^{\bullet+}$ at these wavelengths (SI Text-3.1). H_2O_2 was quantified by the horseradish peroxidase (HRP)-catalyzed oxidation of ABTS to $ABTS^{\bullet+}$ by H_2O_2 (H_2O_2 + 2ABTS → $2ABTS^{\bullet+}$, the HRP-ABTS method). The method has been tested in various matrix compositions including samples of the ferrate(VI)-ABTS reaction and showed accurate quantifications of H_2O_2. For

dx.doi.org/10.1021/es500804g | Environ. Sci. Technol. 2014, 48, 5154−5162

further details of the HRP-ABTS method developed in this study, see SI Text-3.1.

Products from the self-decay of ferrate(VI) were investigated in closed flasks purged with N_2 in buffered solutions at pH 7 and $[Fe(VI)]_0$ = 40−810 μM. After a near completion of the ferrate(VI) self-decay, H_2O_2 and O_2 concentrations were quantified. H_2O_2 was measured by the HRP-ABTS method and aqueous O_2 was determined by a CellOx 325 oxygen electrode with an Oxi 340 m (WTW, Weilheim, Germany). The superoxide radical anion ($O_2^{\bullet-}$) formation was quantified by the tetranitromethane assay.[41] The hydroxyl radical (•OH) formation was checked and quantified by the *para*-chlorobenzoic acid assay[42] and *tert*-butanol assay,[41] respectively. To confirm the oxidation state of iron (Fe(II) or Fe(III)), bypyridine was added to the solution during the self-decay of Fe(VI) and the sample absorbance at 522 nm was measured to selectively determine Fe(II) (bypyridine-Fe(II) complex: ε = 8650 M^{-1} cm^{-1}).[43] For further details, see SI Text-3.2.

To determine the stoichiometry of the ferrate(VI)-Fe(II) reaction, 55 μM of Fe(II) was prepared in a N_2-purged solution buffered with 5 mM carbonate at pH 6.8 and reacted with ferrate(VI) in the concentration range of 0−40 μM. After a few seconds, the remaining Fe(II) was determined by the ferrozine method[44] (see SI Text-3.3).

Self-decay of ferrate(VI) and formation of H_2O_2 at pH 7 were measured as a function of the reaction time at various initial ferrate(VI) and H_2O_2 concentrations. These data were used to validate the ferrate(VI) self-decay kinetic model.

Kinetic Simulation. Kintecus,[45] a chemical kinetic simulator, was used to simulate the reaction of ferrate(VI) with ABTS, ferrate(VI) self-decay, and the reaction of ferrate(VI) with H_2O_2 (see SI Text-4).

RESULTS AND DISCUSSION

Reaction of Ferrate(VI) with ABTS. *Kinetics.* The reaction of ferrate(VI) with ABTS was determined to be first order with respect to each reactant (SI Figures SI-1 and SI-2). Figure 1 shows the apparent second-order rate constants ($k_{app\text{-}ABTS}$) for the reaction of ferrate(VI) with ABTS as a function of pH (1.5−10). The pH dependence of $k_{app\text{-}ABTS}$ can be explained considering the speciation of ferrate(VI) (eqs 1−3), the speciation of ABTS (eq 4), and the eight reactions between the four ferrate(VI) species and the two ABTS species.[46]

$$HABTS^+ \rightleftharpoons ABTS + H^+ \quad pK_4 = 2.1^{46} \tag{4}$$

Accordingly, $k_{app\text{-}ABTS}$ is given by

$$k_{app\text{-}ABTS} = \sum_{j=1,2}^{i=1,2,3,4} k_{ABTS\text{-}i,j}\alpha_i\beta_j$$

where α_i and β_j represent the respective fractions of ferrate(VI) and ABTS present as the species i and j at a given pH, and $k_{ABTS\text{-}i,j}$ represents the species-specific second-order rate constant for each i and j pair. The $k_{ABTS\text{-}i,j}$ were determined by a nonlinear least-squares regression of our experimental data ($k_{app\text{-}ABTS}$) with the constraint of $k_{ABTS\text{-}1,2} \geq k_{ABTS\text{-}2,2} \geq k_{ABTS\text{-}3,2} \geq k_{ABTS\text{-}4,2}$. The constraint is based on the enhanced reactivity of ferrate(VI) species upon protonation due to a decreased electron density on the iron center,[47] which has been observed in many previous studies.[19,20] The regression results showed that in the tested pH range 1−10, the overall reaction is mainly controlled by reactions 5−8. The contribution of the reactions of $H_2Fe^{VI}O_4$ and $HFe^{VI}O_4^-$ with $HABTS^+$ to the overall reaction was much smaller compared to reactions 5−8 due to a smaller overlap of these species at a given pH. The reaction of $Fe^{VI}O_4^{2-}$ with ABTS is also found to be negligible due to lower reactivity of $Fe^{VI}O_4^{2-}$ compared to $HFe^{VI}O_4^-$, which has been observed in previous studies.[4,6,9]

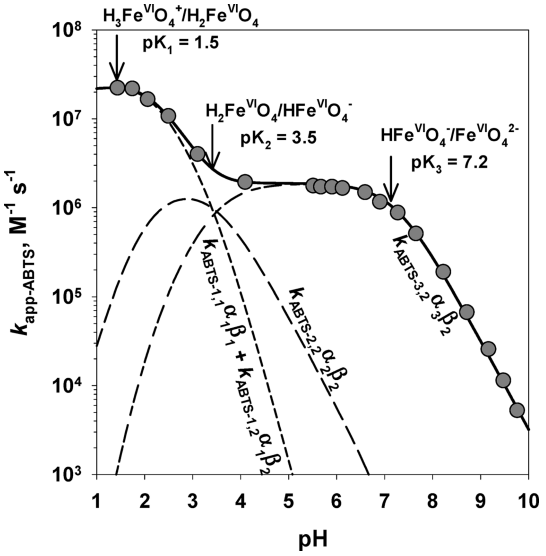

Figure 1. Apparent second-order rate constants ($k_{app\text{-}ABTS}$) for the reaction of ferrate(VI) with ABTS in the pH-range 1.5−10 (25 °C). The symbols represent measured data and the lines represent model calculations. The lines represent the contribution of the reaction of $H_3Fe^{VI}O_4^+$ with $HABTS^+$/ABTS ($k_{ABTS\text{-}1,1}\alpha_1\beta_1 + k_{ABTS\text{-}1,2}\alpha_1\beta_2$, short dashed), $H_2Fe^{VI}O_4$ with ABTS ($k_{ABTS\text{-}2,2}\alpha_2\beta_2$, long dashed) and $HFe^{VI}O_4^-$ with ABTS ($k_{ABTS\text{-}3,2}\alpha_3\beta_2$, short−long dashed) to the overall reaction as a function of pH.

$$H_3Fe^{VI}O_4^+ + HABTS^+ \rightarrow \text{products} \quad k_{ABTS-1,1} \tag{5}$$

$$H_3Fe^{VI}O_4^+ + ABTS \rightarrow \text{products} \quad k_{ABTS-1,2} \tag{6}$$

$$H_2Fe^{VI}O_4 + ABTS \rightarrow \text{products} \quad k_{ABTS-2,2} \tag{7}$$

$$HFe^{VI}O_4^- + ABTS \rightarrow \text{products} \quad k_{ABTS-3,2} \tag{8}$$

The determined rate constants are $k_{ABTS\text{-}1,1} = (1.97 \pm 0.48) \times 10^7$ M^{-1} s^{-1}, $k_{ABTS\text{-}1,2} = (1.19 \pm 0.13) \times 10^8$ M^{-1} s^{-1}, $k_{ABTS\text{-}2,2} = (1.90 \pm 0.54) \times 10^6$ M^{-1} s^{-1}, and $k_{ABTS\text{-}3,2} = (1.90 \pm 0.04) \times 10^6$ M^{-1} s^{-1}. Based on the obtained species specific rate constants, the contribution of each reaction (i.e., reactions 5−8) to the overall reaction rate was calculated (Figure 1, dashed lines).

Products and Stoichiometry. The reduction of ferrate(VI) to Fe(III) as a final product requires three-electron equivalents and the oxidation of ABTS to $ABTS^{\bullet+}$ generates a one-electron equivalent. Therefore, one mole of ferrate(VI) can theoretically oxidize three moles of ABTS and generate three moles of $ABTS^{\bullet+}$. However, Figure 2 shows that one mole of ferrate(VI) oxidized only one mole of ABTS (slope = 0.97) and generates one mole of $ABTS^{\bullet+}$ (0.99) when 0−24 μM of ferrate(VI) react with 80 μM of ABTS at pH 2.9. The missing two-electron equivalents can be explained by the formation of H_2O_2 with a stoichiometry close to 1 (0.93) for the H_2O_2 formation and ferrate(VI) consumption (Figure 2).

The stoichiometry for the reaction between ferrate(VI) and ABTS was also measured at different pH values. Figure 3 shows

dx.doi.org/10.1021/es500804g | Environ. Sci. Technol. 2014, 48, 5154−5162

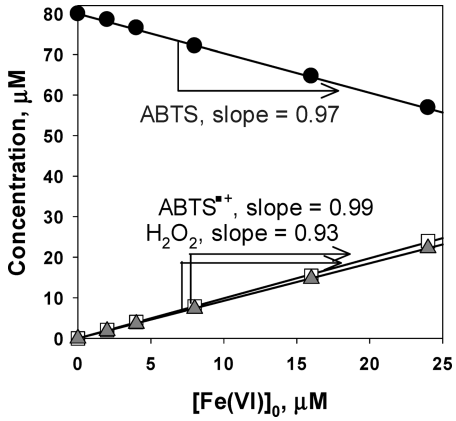

Figure 2. Reaction of ferrate(VI) with ABTS at pH 2.9. Consumption of ABTS (solid circles) and formation of $ABTS^{\bullet+}$ (empty squares) and H_2O_2 (gray triangles) as a function of the initial ferrate(VI) concentration. Consumption of ABTS and formation of $ABTS^{\bullet+}$ and H_2O_2 were measured for each ferrate(VI) dose after complete consumption of ferrate(VI). Experimental conditions: $[Fe(VI)]_0$ = 0–24 μM and $[ABTS]_0$ = 80 μM.

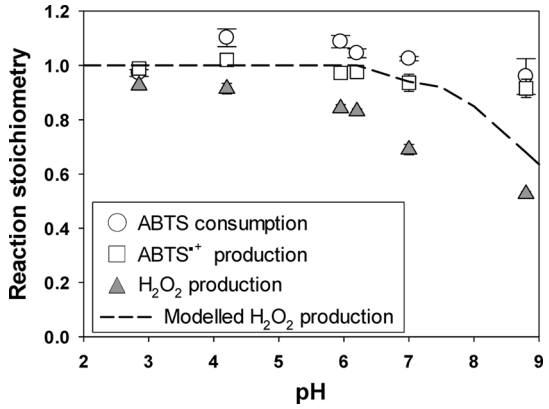

Figure 3. pH-dependent reaction stoichiometry for the consumption of ABTS and the production of $ABTS^{\bullet+}$ and H_2O_2 from the reaction of ferrate(VI) with ABTS. $[Fe(VI)]_0$ = 0–24 μM and $[ABTS]_0$ = 80 μM. Symbols represent the measured data and the dash line represents the modeled H_2O_2 production (see text). Error bars represent one standard deviation of data.

that within the investigated pH range of 2.9–8.8, one mole of ferrate(VI) consumed one mole of ABTS (0.96–1.09) and generated one mole of $ABTS^{\bullet+}$ (0.92–1.02). However, the yield of H_2O_2 decreased from 0.93 to 0.53 with increasing pH from 2.9 to 8.8. Possible reasons for H_2O_2 yields <1 will be discussed below.

Mechanism. Based on our observations, eqs 9–12 in Table 1 and Scheme 1 are proposed as the major reactions for the ferrate(VI)-ABTS system in phosphate buffered solution. The iron and ABTS species are expressed considering only the major species at pH 7.

The reaction of $HFe^{VI}O_4^-$ with ABTS proceeds via a one-electron transfer process and produces $H_2Fe^{V}O_4^-$ and $ABTS^{\bullet+}$ as primary products (reaction 9). This is supported by the quantitative formation of $ABTS^{\bullet+}$ from the reaction of ferrate(VI) with ABTS with a stoichiometry of 1 (Figure 2). The $k_{app\text{-}ABTS}$ shown in Figure 1 corresponds to k_9 because the rate constants were determined by monitoring the formation of $ABTS^{\bullet+}$. The produced perferryl(V) ($H_2Fe^{V}O_4^-$) has three competing pathways, (reactions 10–12). Perferryl(V) has been known to self-decay by first-order (eq 10) or second-order (eq 11) kinetics depending on pH and perferryl(V) concentration.[34,35] In both pathways, the products of perferryl(V) decay are Fe(III) and H_2O_2. At acidic pH, it is proposed that perferryl(V) decays mainly via eq 10 or 11 to Fe(III) ($Fe^{III}(OH)_3$ (aq)) and H_2O_2. The combination of eqs 9 and 10 or eqs 9 and 11 results in the net reaction: $HFe^{VI}O_4^- + ABTS + H_2O + 2H^+ \rightarrow Fe^{III}(OH)_3 + ABTS^{\bullet+} + H_2O_2$, which is consistent with the observed 1:1 reaction stoichiometry for H_2O_2 formation at pH $\leq$ 4.2 (Figure 3). As the pH increases over 4.2, the reaction of perferryl(V) with H_2O_2 (eq 12) can compete with the perferryl(V) self-decay reactions (eqs 10 and 11) as the rates of the latter two reactions decrease significantly with increasing pH while the rate of reaction 12 remains almost constant (SI Figure SI-15). Reaction 12 produces Fe(III) and O_2, which explains the decrease of the H_2O_2 yield with increasing pH (Figure 3).

Kinetic Simulation. The rate constants, k_{10}, k_{11}, and k_{12} have been determined previously using a premix pulse-radiolysis technique.[21,34,35] As all the kinetic information is available for reactions 9–12 (SI Figure SI-15), the proposed ferrate(VI)-ABTS reaction system can be kinetically modeled (SI Text-4.1). The model was used to simulate the H_2O_2 yields from the reaction of ferrate(VI) with ABTS as a function of pH. Figure 3

Table 1. Major Reactions for the Ferrate(VI)-ABTS System (Eqs 9–12) and the Self-Decay of Ferrate(VI) (Eqs 10 and 2–16) in a Phosphate-Buffered Solution at pH 7

eq	reactions	k at pH 7
9	$HFe^{VI}O_4^- + ABTS + H^+ \rightarrow H_2Fe^{V}O_4^- + ABTS^{\bullet+}$	1.2×10^6 M^{-1} s^{-1} [a]
10	$H_2Fe^{V}O_4^- + H_2O + H^+ \rightarrow Fe^{III}(OH)_3(aq) + H_2O_2$	10^2 M^{-1} s^{-1} [b]
11	$2H_2Fe^{V}O_4^- + 2H_2O + 2H^+ \rightarrow 2Fe^{III}(OH)_3(aq) + 2H_2O_2$	5.8×10^7 M^{-1} s^{-1} [c]
12	$H_2Fe^{V}O_4^- + H_2O_2 + H^+ \rightarrow Fe^{III}(OH)_3(aq) + O_2 + H_2O$	5.6×10^5 M^{-1} s^{-1} [d]
13	$2HFe^{VI}O_4^- + 4H_2O \rightarrow 2H_3Fe^{IV}O_4^- + 2H_2O_2$	26 M^{-1} s^{-1} [e]
14	$H_3Fe^{IV}O_4^- + H_2O_2 + H^+ \rightarrow Fe^{II}(OH)_2(aq) + O_2 + 2H_2O$	$\sim 10^4$ M^{-1} s^{-1} [f]
15	$HFe^{VI}O_4^- + Fe^{II}(OH)_2(aq) + H_2O \rightarrow H_2Fe^{V}O_4^- + Fe^{III}(OH)_3(aq)$	$\sim 10^7$ M^{-1} s^{-1} [g]
16	$HFe^{VI}O_4^- + H_2O_2 \rightarrow H_3Fe^{IV}O_4^- + O_2$	10 M^{-1} s^{-1} [h]

[a]This study (Figure 1). [b]Rush and Bielski,[35] [c]Rush and Bielski,[34] [d]Rush et al.,[21] [e]This study (Figure 4). [f]This study (estimated, see main text). [g]This study (see SI Text-2.4). [h]This study (SI Figure SI-9).

dx.doi.org/10.1021/es500804g | Environ. Sci. Technol. 2014, 48, 5154–5162

Scheme 1. Reaction Scheme for the Reaction of Ferrate(VI) with ABTS[a]

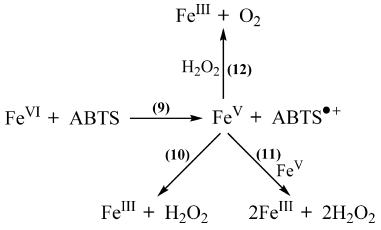

[a]The numbers in brackets correspond to the reactions in Table 1.

and SI Figure SI-16 show that the behavior of the pH-dependent H_2O_2 yield (i.e., decreasing H_2O_2 yield from 0.93 to 0.53 with increasing pH from 2.9 to 8.8) can be reasonably simulated by the kinetic model albeit the predicted H_2O_2 yields were higher than the measured ones by 7% (pH 2.9) to 26% (pH 8.8) in the investigated pH range. This level of deviations is acceptable considering the uncertainty of each rate constant (eqs 9−12), which were determined under different experimental conditions.

Reaction of Ferrate(VI) with Ferrate(VI) (Self-Decay of Ferrate(VI)). *Kinetics.* The self-decay of ferrate(VI) followed second-order kinetics with respect to ferrate(VI) (SI Figures SI-3 and SI-5). Figure 4 shows the apparent second-order rate constants ($k_{app\text{-}self}$) for the self-decay of ferrate(VI) in the pH range of 1−8.2, which were determined by measuring the ferrate(VI) decrease either by monitoring the absorbance at 510 nm (filled circles) or by the ABTS method (empty triangles). The two methods gave consistent $k_{app\text{-}self}$ values in the pH range 3−8. The $k_{app\text{-}self}$ values show a strong pH-dependence and increase more than 4 orders of magnitude with a decrease of the pH from 8 to 2. The pH dependence of $k_{app\text{-}self}$ can be explained by considering the following reactions among ferrate(VI) species (eqs 17−22). The reaction between fully deprotonated ferrate(VI) species (i.e., $Fe^{VI}O_4^{2-} + Fe^{VI}O_4^{2-} \rightarrow$) was found to contribute negligibly to the overall reaction.

$$H_3Fe^{VI}O_4^{+} + H_3Fe^{VI}O_4^{+} \rightarrow \text{products} \quad k_{self\text{-}1,1} \tag{17}$$

$$H_3Fe^{VI}O_4^{+} + H_2Fe^{VI}O_4 \rightarrow \text{products} \quad k_{self\text{-}1,2} \tag{18}$$

$$H_2Fe^{VI}O_4 + H_2Fe^{VI}O_4 \rightarrow \text{products} \quad k_{self\text{-}2,2} \tag{19}$$

$$H_2Fe^{VI}O_4 + HFe^{VI}O_4^{-} \rightarrow \text{products} \quad k_{self\text{-}2,3} \tag{20}$$

$$HFe^{VI}O_4^{-} + HFe^{VI}O_4^{-} \rightarrow \text{products} \quad k_{self\text{-}3,3} \tag{21}$$

$$HFe^{VI}O_4^{-} + Fe^{VI}O_4^{2-} \rightarrow \text{products} \quad k_{self\text{-}3,4} \tag{22}$$

Accordingly, $k_{app\text{-}self}$ is given by

$$k_{app\text{-}self} = \sum_{j=1,2,3}^{i=1,2,3,4} k_{self\text{-}i,j}\alpha_i\alpha_j$$

where α_i or α_j represent the fraction of the ferrate(VI) species and $k_{self\text{-}i,j}$ represent the species-specific second-order rate constants for the reaction between ferrate(VI) species i and j. $k_{self\text{-}i,j}$ values were determined by a nonlinear least-squares regression of the pH-dependent $k_{app\text{-}self}$ values. The determined rate constants were $k_{self\text{-}1,1} = (1.01 \pm 0.22) \times 10^6\ M^{-1}\ s^{-1}$, $k_{self\text{-}1,2} = (5.13 \pm 1.28) \times 10^5\ M^{-1}\ s^{-1}$, $k_{self\text{-}2,2} = (3.68 \pm 0.61) \times 10^4\ M^{-1}\ s^{-1}$, $k_{self\text{-}2,3} = (1.07 \pm 0.15) \times 10^4\ M^{-1}\ s^{-1}$, $k_{self\text{-}3,3} = (1.19 \pm 0.09) \times 10^2\ M^{-1}\ s^{-1}$, and $k_{self\text{-}3,4} = (2.38 \pm 0.41) \times 10\ M^{-1}\ s^{-1}$. Protonation of ferrate(VI) species significantly enhances the rate of the ferrate(VI) self-decay. The contribution of each ferrate(VI) species to the overall self-decay rate of ferrate(VI) was also calculated (Figure 4, dashed lines).

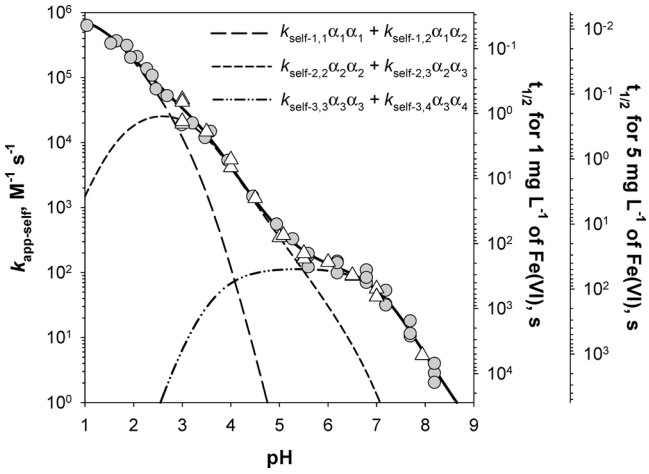

Figure 4. Apparent second-order rate constants ($k_{app\text{-}self}$, left-axis) and half-lives ($t_{1/2}$, right-axis) for the self-decay of ferrate(VI) as a function of pH (1.0−8.2) at T = 24 ± 1 °C. Symbols: measured data; lines: model calculations. The $k_{app\text{-}self}$ values were obtained from ferrate(VI) decrease monitored at 510 nm (circles) or by the ABTS method (triangles). The half-lives are calculated for initial ferrate(VI) concentrations of 1 and 5 mg Fe L^{-1} ($[Fe(VI)]_0$ = 18 and 90 μM), respectively, based on $t_{1/2} = 1/(2k_{app\text{-}self}[Fe(VI)]_0)$. The dashed lines represent the contribution of the reactions of $H_3Fe^{VI}O_4^{+}$ with $H_3Fe^{VI}O_4^{+}/H_2Fe^{VI}O_4$ ($k_{self\text{-}1,1}\alpha_1\alpha_1 + k_{self\text{-}1,2}\alpha_1\alpha_2$, long dashed) $H_2Fe^{VI}O_4$ with $H_2Fe^{VI}O_4/HFe^{VI}O_4^{-}$ ($k_{self\text{-}2,2}\alpha_2\alpha_2 + k_{self\text{-}2,3}\alpha_2\alpha_3$, short dashed) and $HFe^{VI}O_4^{-}$ with $HFe^{VI}O_4^{-}/Fe^{VI}O_4^{2-}$ ($k_{self\text{-}3,3}\alpha_3\alpha_3 + k_{self\text{-}3,4}\alpha_3\alpha_4$, dashed-dotted) to the overall reaction as a function of pH.

Since the self-decay of ferrate(VI) follows second-order kinetics with respect to ferrate(VI), the half-lives for ferrate(VI) decay ($t_{1/2}$) depend on the initial concentration of ferrate(VI): $t_{1/2} = 1/(2k_{app\text{-}self}[Fe(VI)]_0)$. Figure 4 shows the calculated $t_{1/2}$ for initial ferrate(VI) concentrations of 1 and 5 mg Fe L^{-1} ($[Fe(VI)]_0$ = 18 and 90 μM), respectively. The $t_{1/2}$ strongly depends on pH and initial ferrate(VI) concentration. For an increase of pH from 7 to 8 (typical pH ranges of natural waters, drinking waters and wastewaters), $t_{1/2}$ increases from 470 to 4310 s for an initial ferrate(VI) concentration of 1 mg Fe L^{-1}. For an initial ferrate(VI) concentration of 5 mg Fe L^{-1}, $t_{1/2}$ was 90 and 860 s at pH 7 and 8, respectively. Therefore, ferrate(VI) disappears in a few minutes at pH 7 and ferrate(VI) doses of >5 mg Fe L^{-1}, but is stable for a few hours at pH 8 and ferrate(VI) doses of <1 mg Fe L^{-1}.

Products. Most experiments for elucidating products from ferrate(VI) self-decay were performed in phosphate buffered solutions at pH 7. In this study, H_2O_2, O_2 and Fe(III) were identified and quantified as major stable products from ferrate(VI) self-decay. The formation of H_2O_2 from self-decay of ferrate(VI) has not been reported nor quantified so far even though H_2O_2 formation has been reported from self-decay of perferryl(V)[34,35] or ferryl(IV)[36] species. Figure 5 shows the measured formation of H_2O_2 and O_2 after near complete decay of ferrate(VI) (>95%) at pH 7 as a function of the initial ferrate(VI) concentration. The average yield (molar ratio based on the initial ferrate(VI)) at pH 7 and $[Fe(VI)]_0$ = 40−810 μM

dx.doi.org/10.1021/es500804g | Environ. Sci. Technol. 2014, 48, 5154−5162

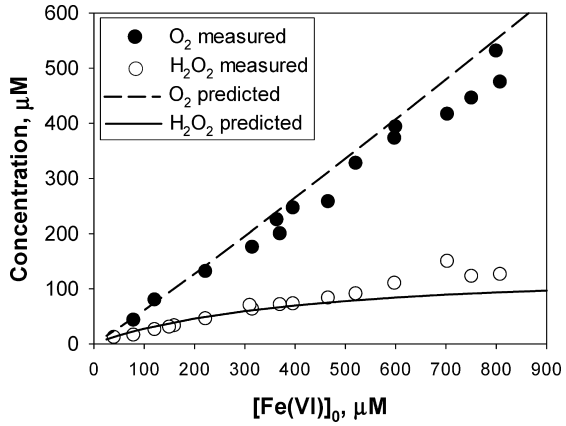

Figure 5. Formation of O_2 and H_2O_2 from the self-decay of ferrate(VI) as a function of the initial ferrate(VI) concentration in phosphate buffered solution at pH 7 (10 mM for $[Fe(VI)]_0 < 300$ μM and 100 mM for $[Fe(VI)]_0 \geq 300$ μM). H_2O_2 and O_2 were determined when most of the added Fe(VI) was depleted (>95%). The symbols represent measured data and the lines model calculations with the reactions shown in Scheme 2

was determined to be 21 ± 3% for H_2O_2 and 60 ± 4% for O_2. H_2O_2 was also formed at acidic pH and the average yield was 31 ± 3% at pH 3.3 and $[Fe(VI)]_0 = 2.5-150$ μM (SI Figure SI-17). Kinetic simulations at pH 7 (see below for details) showed that the yield of H_2O_2 decreases gradually from 33% at $[Fe(VI)]_0 = 25$ μM to 11% at $[Fe(VI)]_0 = 900$ μM (SI Figure SI-17). The final oxidation-state of the iron species was checked by using bipyridine which forms a strong red-colored complex with Fe(II).[43] Since no Fe(II)-bipyridine was detected upon addition of 100 μM of bipyridine to the reaction solution, it can be concluded that Fe(III) is the final product from ferrate(VI) self-decay.

The formation of $O_2^{\bullet-}$ was checked using a tetranitromethane assay.[41] $O_2^{\bullet-}$ reacts very rapidly with tetranitromethane ($C(NO_2)_4$) and produces the nitroform anion ($C(NO_2)_3^-$): $O_2^{\bullet-} + C(NO_2)_4 \rightarrow O_2 + C(NO_2)_3^- + NO_2^{\bullet}$, $k = 2 \times 10^9$ M^{-1} s^{-1}.[41] By measuring the light absorption at 350 nm where the nitroform anion shows a maximum (ε = 15 000 M^{-1} cm^{-1} [41]), the formation of $O_2^{\bullet-}$ can be quantified. The result showed that a negligible concentration of $O_2^{\bullet-}$ was formed (<2%) for the ferrate(VI) self-decay ($[Fe(VI)]_0 = 40$ μM) at pH 7 (SI Figure SI-12).

The formation of $^{\bullet}OH$ was examined by the transformation of *para*-chlorobenzoic acid (*p*CBA) which has been widely used as an $^{\bullet}OH$-probe compound in ozonation systems.[42] Transformation of *p*CBA (1 μM) was tested at pH 7 during self-decay of ferrate(VI) with initial concentrations of 25, 50, and 100 μM. The *p*CBA transformation was less than 3%, indicating a very low yield for $^{\bullet}OH$ from the ferrate(VI) self-decay. The formation of $^{\bullet}OH$ was also quantified by measuring formaldehyde formation in the presence of an excess of *tert*-butanol.[41] In excess of *tert*-butanol (1 mM in this study), most $^{\bullet}OH$, if produced, react with *tert*-butanol ($k = 6 \times 10^8$ M^{-1} s^{-1})[41] producing several products including formaldehyde. Therefore, by measuring formaldehyde, the $^{\bullet}OH$ formation can be estimated. The results showed that $^{\bullet}OH$ yields ($=\Delta[^{\bullet}OH]/\Delta[Fe(VI)] \times 100$) from the self-decay of ferrate(VI) at pH 7 are less than 5% (SI Figure SI-13).

Mechanism. Equations 10 and 12−16 in Table 1 and Scheme 2 are proposed as the major reactions and the reaction sequence responsible for the self-decay of ferrate(VI) at pH 7 in phosphate buffered solution.

Scheme 2. Reaction Scheme for the Self-Decay of Ferrate(VI)[a]

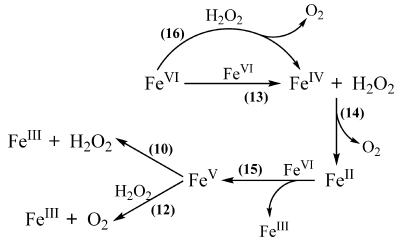

[a]The numbers in the brackets correspond to the reactions in Table 1.

Reaction 13 represents the initiation of ferrate(VI) self-decay in which two ferryl(IV) and two H_2O_2 are produced from the reaction of two ferrate(VI). Scheme 3 shows the reaction mechanism proposed for reaction 13 in detail. The reaction starts with dimerization of two ferrate(VI) to form a diferrate(VI) intermediate ($-Fe^{VI}-O-Fe^{VI}-$), which subsequently undergoes intramolecular oxo-coupling via a two-electron transfer. The oxo-coupled diferrate(V) then transforms into diferrate(V) ($-Fe^{V}-O-Fe^{V}-$) liberating H_2O_2 by two consecutive hydrolysis steps. The diferrate(V) undergoes a similar intramolecular oxo-coupling and subsequent hydrolysis generates diferrate(IV) ($-Fe^{IV}-O-Fe^{IV}-$) and H_2O_2. Finally, the diferrate(IV) is hydrolyzed into two ferryl(IV) species.

The formation of diferrate(VI) species has also been proposed as the initial step in the ferrate(VI) self-decay mechanism in strong acidic solution (pH ~ 1),[39] which was based on experimental (competitive ^{18}O kinetic isotope effect) and computational studies (DFT analysis of a peroxide bond formation). However, direct O_2 formation was proposed in acidic solutions by a four-electron reduction of the oxide-ligands of diferrate(VI). This mechanism for direct O_2 formation without involvement of H_2O_2 is not consistent with our data showing significant H_2O_2 formation at pH 7.0 as well as pH 3.3 (SI Figure SI-17).

The second-order rate constant for reaction 13 (k_{13}) should correspond to the initial dimerization rate of ferrate(VI), which is consistent with the observed second-order kinetics for ferrate(VI) self-decay with respect to the ferrate(VI) concentration. k_{13} is proposed to be one-half of the experimentally determined apparent ferrate(VI) self-decay rate constant (i.e., $2k_{13} \approx k_{app,self} = 52$ M^{-1} s^{-1} at pH 7). This is based on the assumption that the overall reaction is dominated by reactions 13, 14, 15, and 10 during the initial phase of the ferrate(VI) self-decay when H_2O_2 formation is still low. Under those conditions, the sum of reactions 13, 14, 15, and 10 results in $4Fe(VI) \rightarrow 4Fe(III) + 2H_2O_2 + 2O_2$ (see Scheme 2). Therefore, four ferrate(VI) are consumed per each onset of reaction 13.

The ferryl(IV) produced from reaction 13 reacts mainly with H_2O_2 which produces Fe(II) and O_2 (reaction 14) via a concerted two-electron transfer. Ferryl(IV) could react with H_2O_2 via two consecutive one-electron transfers involving $O_2^{\bullet-}$ as an intermediate. However, our measurements show quite low $O_2^{\bullet-}$ yields (<2%) during ferrate(VI) self-decay, which supports the concerted two-electron transfer mechanism.

dx.doi.org/10.1021/es500804g | Environ. Sci. Technol. 2014, 48, 5154−5162

Scheme 3. Proposed Mechanism for the Initiation of Ferrate(VI) Self-Decay (Reaction 13)

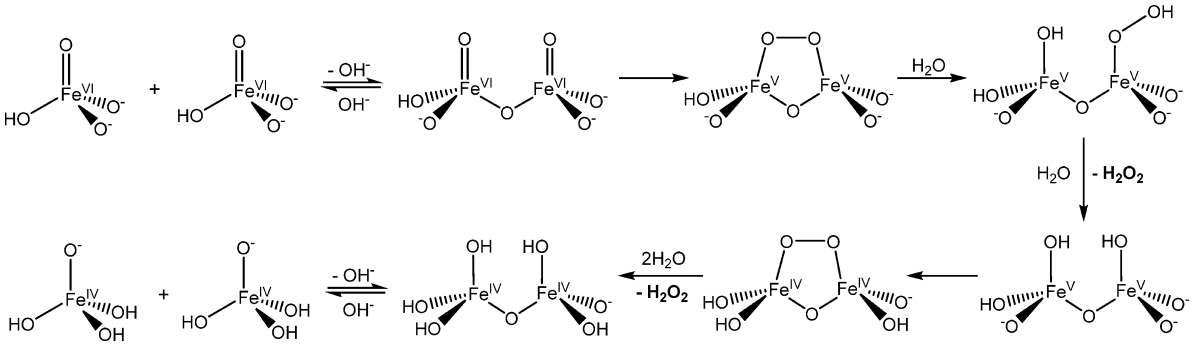

So far, kinetic information for the aqueous ferryl(IV) reactions was available only at acidic (pH < 3)[28−32] or basic pH (pH > 10)[27,36] conditions but not in the pH range 3−10. The second-order rate constant for the reaction of ferryl(IV) with H_2O_2 was determined to be 1×10^4 M^{-1} s^{-1} in 1 M $HClO_4$[28] and 3.9×10^5 M^{-1} s^{-1} at pH 10.[36] This difference in the rate constant is attributable to the different pH-dependent ferryl(IV) (currently information is not available) and H_2O_2 speciation ($H_2O_2 \rightleftharpoons HO_2^- + H^+$) involved in the reactions. Our kinetic simulations showed that the kinetics of O_2 and H_2O_2 formation is independent of the magnitude of k_{14} as long as $k_{14} \geq 10^4$ M^{-1} s^{-1}. This can be explained by the fact that reaction 14 is the sole reaction pathway for ferryl(IV) in our kinetic model. Therefore, a value of 10^4 M^{-1} s^{-1} was used in the subsequent kinetic simulations. The k_{14} value can also be estimated by considering the two-orders of magnitude larger reactivity of ferryl(IV) than ferrate(VI) or two-orders of magnitude smaller reactivity of ferryl(IV) than perferryl(V) observed in some kinetic studies.[27] The second-order rate constants at pH 7 for the reaction of H_2O_2 with ferrate(VI) and perferryl(V) was 21 M^{-1} s^{-1} (see SI Figure SI-9) and 5.6×10^5 M^{-1} s^{-1},[21] respectively. Based on this, a k_{14} value of $\sim 5 \times 10^3$ M^{-1} s^{-1} is estimated.

Fe(II) produced from reaction 14 is proposed to be oxidized by ferrate(VI) via a one-electron transfer generating perferryl-(V) and Fe(III) as products (reaction 15). The stoichiometry and kinetics of reaction 15 were investigated in this study. SI Figure SI-14 shows that 3 mol of Fe(II) are consumed per mole of ferrate(VI) during oxidation of 56 μM of Fe(II) by ferrate(VI) (0−20 μM) in 5 mM carbonate solution at pH 6.8. This 3:1 stoichiometry for Fe(II):ferrate(VI) is consistent with an initial one-electron oxidation of Fe(II) by ferrate(VI) (reaction 15) and subsequent two additional oxidation steps of Fe(II) by perferryl(V) and ferryl(IV), respectively, in which the latter two species are produced from consecutive one-electron reduction of ferrate(VI). The second-order rate constant for reaction 15 (k_{15}) was found to be higher than 5×10^6 M^{-1} s^{-1} at pH 5 from a kinetic experiment using stopped-flow (SI Text-2.4). Kinetic simulations showed that the kinetics of O_2 and H_2O_2 formation are independent of the magnitude of k_{15} if it is larger than 5×10^6 M^{-1} s^{-1}. A value of 10^7 M^{-1} s^{-1} was used for k_{15} at pH 7 as a lower limit in the kinetic simulations. The second-order rate constant for the reaction of ferrate(VI) with Fe(II) was reported to be 10^5 M^{-1} s^{-1} at pH 12 in which $Fe^{VI}O_4^{2-}$ and $Fe^{II}(OH)_2$ are the major species.[48] It is difficult to compare the rate constant determined at pH 12 directly to our value because the reactivity of Fe(VI) and Fe(II) depends strongly on their pH-dependent speciation. The reaction of Fe(II) with ferrate(VI) can also be compared to the ferrate(VI) reaction with ferrocyanide ($[Fe^{II}(CN)_6]^{4-}$) and pentacyanoaquaferrate(II) ($[Fe^{II}(CN)_5(H_2O)]^{3-}$).[49] The second-order rate constants for the reaction of $HFe^{VI}O_4^-$ were 3.0 $\times 10^5$ M^{-1} s^{-1} for ferrocyanide and 3.5×10^8 M^{-1} s^{-1} for pentacyanoaquaferrate(II), respectively. A 3:1 reaction stoichiometry was also observed for both $[Fe^{II}(CN)_6]^{4-}$:Fe(VI) and $[Fe^{II}(CN)_5(H_2O)]^{3-}$:Fe(VI) couples.[49] Finally, kinetic simulations show that the oxidation of Fe(II) by perferryl(V) or ferryl(IV) is not important during ferrate(VI) self-decay due to the rapid oxidation of Fe(II) by ferrate(VI) (see SI Text-4.2 for further discussions).

Perferryl(V) produced from reaction 15 has two major reaction pathways, that is, reactions 10 and 12 (Scheme 2), which were described in an earlier section for the reaction mechanism of the Fe(VI)-ABTS system. Reaction 10 represents the self-decay of perferryl(V) with first-order kinetics generating Fe(III) and H_2O_2 ($k_{10} = 10^2$ s^{-1} at pH 7).[35] Another reaction pathway of perferryl(V) is its reaction with H_2O_2, which generates Fe(III) and O_2 via a two-electron transfer (reaction 12, $k_{12} = 5.6 \times 10^5$ M^{-1} s^{-1} at pH 7).[21] The self-decay of perferryl(V) with second-order kinetics (i.e., reaction 11, Table 1) was not included in the ferrate(VI) self-decay model for pH 7 because its removal from the kinetic model causes little change in the concentration profiles which was found from the model sensitivity analysis (data not shown).

Reaction 16 represents the oxidation of H_2O_2 by ferrate(VI) via a two-electron transfer, generating ferryl(IV) and O_2, which has been proposed previously.[21,27] A one-electron transfer process would have resulted in significant $O_2^{\bullet-}$ formation, which is not consistent with our observations. The second-order rate constant for reaction 16 (k_{16}) was investigated in this study within the pH range 7−12 (SI Figure SI-9). The apparent k-value for the decrease of ferrate(VI) in the presence of excess H_2O_2 ($k_{app\text{-}H2O2}$) was determined to be 20 M^{-1} s^{-1} at pH 7. In excess of H_2O_2 over ferrate(VI), two moles of ferrate(VI) can be consumed per every event of reaction 16 as the ferryl(IV) produced from reaction 16 will generate Fe(II) by reaction 14, which in turn will consume another ferrate(VI) by reaction 15. Perferryl(V) from reaction 15 will then be converted into Fe(III) and H_2O_2 (reaction 11) or Fe(III) and O_2 (reaction 12) as final products (Scheme 2). Therefore, k_{16} should be one-half of the apparent second-order rate constant that are measured in excess of H_2O_2 (i.e., $k_{app\text{-}H2O2} = 2k_{16}$) and a value of 10 M^{-1} s^{-1} at pH 7 was used in the kinetic simulations.

Kinetic Simulations. A kinetic model based on reactions 10 and 12−16 in Table 1 (or Scheme 2) was used to simulate the behavior of ferrate(VI) self-decay under various experimental

dx.doi.org/10.1021/es500804g | Environ. Sci. Technol. 2014, 48, 5154−5162

conditions. Figure 5 shows that the formation of O_2 and H_2O_2 from the self-decay of ferrate(VI) as a function of the initial ferrate(VI) concentration could be successfully predicted using this kinetic model. Figure 6 shows the time-dependent concentration changes of ferrate(VI) and H_2O_2 during the self-decay of ferrate(VI) at pH 7 for varying initial ferrate(VI) concentrations, $[Fe(VI)]_0$ = (a) 10, (b) 40, (c) 150, and (d) 310 μM. With increasing initial ferrate(VI) concentrations, the ferrate(VI) self-decay rate increases, which reflects the second-order nature of this reaction. The H_2O_2 yield ($=\Delta[H_2O_2]/\Delta[Fe(VI)]$) was ~28% for $[Fe(VI)]_0$ = 10 and 40 μM and decreased to ~21% for $[Fe(VI)]_0$ = 150 and 310 μM. The data clearly show that the concentration profiles of ferrate(VI) and H_2O_2 can be successfully predicted by the kinetic model.

The kinetic model was also applied to simulate the reaction of ferrate(VI) with H_2O_2 at pH 7. SI Figure SI-18 shows the measured and predicted ferrate(VI) and H_2O_2 concentrations as a function of the reaction time during the reaction of 40 μM ferrate(VI) with H_2O_2 for three different initial H_2O_2 concentrations: (a) $[H_2O_2]_0$ = 20 μM, (b) $[H_2O_2]_0$ = 40 μM, and (c) $[H_2O_2]_0$ = 80 μM. While the decrease of ferrate(VI) was nearly completed within 40 min, the H_2O_2 concentration decreased little for $[H_2O_2]_0$ = 40 and 80 μM or slightly increased for $[H_2O_2]_0$ = 20 μM due to the formation of H_2O_2 from the ferrate(VI) self-decay. Overall, the kinetic model based on Scheme 2 predicts successfully the behavior of ferrate(VI) and H_2O_2 during the ferrate(VI) self-decay (Figures 5 and 6) and the reaction of ferrate(VI) with H_2O_2 (SI Figure SI-18).

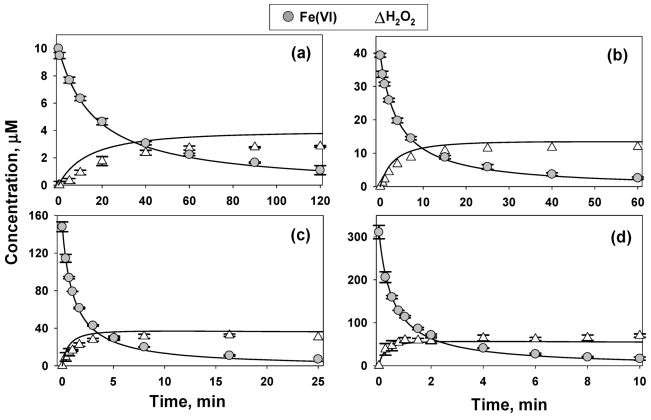

Figure 6. Measured and predicted self-decay of ferrate(VI) and formation of H_2O_2 as a function of the reaction time in a phosphate buffered solution (5 mM) at pH 7 for varying initial ferrate(VI) concentrations, $[Fe(VI)]_0$ = (a) 10, (b) 40, (c) 150, and (d) 310 μM. Symbols: measured data; lines: model calculations. Error bars represent one standard deviation of data.

Implications for Water Treatment with Ferrate(VI). Ferrate(VI) self-decay and ferrate(VI) reaction with water matrix components (e.g., dissolved organic matter) can consume significant amounts of ferrate(VI) during water treatment, which might decrease the treatment efficiency (e.g., elimination of micropollutants). Based on the kinetic information in Figure 4, ferrate(VI) self-decay can be minimized by increasing the pH or lowering the ferrate(VI) dose (e.g., by splitting it into multiple doses in a reactor). However, when adjusting the pH, the decreasing reactivity of ferrate(VI) with target compounds with increasing pH also has to be considered for process optimization. Even though it has been assumed that perferryl(V) or ferryl(IV) produced from ferrate(VI) reactions may enhance the transformation of ferrate(VI)-resistant micropollutants in water treatment, based on our observations, this can result in a much smaller contribution than expected from the theoretical oxidation capacity of ferrate(VI) (i.e., three or four electron equivalents per Fe(VI)) due to the rapid conversion of perferryl(V) into H_2O_2 or the reactions of perferryl(V)/ferryl(IV) with H_2O_2. Finally, a proper management of the residual H_2O_2 after ferrate(VI) treatment process has to be considered. To this end a biological post-treatment could be a good option, which is applied for abatement of H_2O_2, for example, after the UV/H_2O_2 process.

■ ASSOCIATED CONTENT

Supporting Information

Four texts and 18 figures are available for further information addressing materials, experimental procedures and additional data. This material is available free of charge via the Internet at http://pubs.acs.org.

■ AUTHOR INFORMATION

Corresponding Author

*Phone: 41-44-8235270; fax: 41-44-8235210; e-mail: vongunten@eawag.ch.

Notes

The authors declare no competing financial interest.

■ ACKNOWLEDGMENTS

This study was supported by the Swiss Federal Offices for the Environment (07.0142.PJ/I232-2755), and the Basic Science Research Program through the National Research Foundation of Korea (NRF-2012R1A1A1010985) funded by the Ministry of Science ICT & Future Planning. We thank Anh Trung Kieu, Lisa Salhi, and Minju Lee for their contribution to this study.

■ REFERENCES

(1) Ma, J.; Liu, W. Effectiveness and mechanism of potassium ferrate(VI) peroxidation for algae removal by coagulation. *Water Res.* **2002**, *36*, 871−878.

(2) Ma, J.; Liu, W. Effectiveness of ferrate(VI) peroxidation in enhancing the coagulation of surface waters. *Water Res.* **2002**, *36*, 4959−4962.

(3) Lee, Y.; Um, I. H.; Yoon, J. Arsenic(III) oxidation by iron(VI) (ferrate) and subsequent removal of arsenic(V) by iron(III) coagulation. *Environ. Sci. Technol.* **2003**, *37*, 5750−5756.

(4) Lee, Y.; Yoon, J.; von Gunten, U. Kinetics of the oxidation of phenols and phenolic endocrine disruptors during water treatment with ferrate (Fe(VI)). *Environ. Sci. Technol.* **2005**, *39*, 8978−8984.

(5) Sharma, V. K.; Mishra, S. K.; Nesnas, N. Oxidation of sulfonamide antimicrobials by ferrate(VI) [$Fe^{VI}O_4^{2-}$]. *Environ. Sci. Technol.* **2006**, *40*, 7222−7227.

(6) Lee, C.; Lee, Y.; Schmidt, C.; Yoon, J.; von Gunten, U. Oxidation of suspected N-nitrosodimethylamine (NDMA) precursors by ferrate(VI): Kinetics and effect on the NDMA formation potential of natural waters. *Water Res.* **2008**, *42*, 433−441.

(7) Li, C.; Li, X. Z.; Graham, N.; Gao, N. Y. The aqueous degradation of bisphenol-A and steroid estrogens by ferrate. *Water Res.* **2008**, *42*, 109−120.

(8) Hu, L.; Martin, H. M.; Arce-Bulted, O.; Sugihara, M. N.; Keating, K. A.; Strathmann, T. J. Oxidation of carbamazepine by Mn(VII) and Fe(VI): Reaction kinetics and mechanism. *Environ. Sci. Technol.* **2009**, *43*, 509−515.

(9) Lee, Y.; Zimmermann, S. G.; Kieu, A. T.; von Gunten, U. Ferrate (Fe(VI)) application for municipal wastewater treatment: A novel process for simultaneous micropollutant oxidation and phosphate removal. *Environ. Sci. Technol.* **2009**, *43*, 3831−3838.
(10) Noorhasan, N.; Patel, B.; Sharma, V. K. Ferrate(VI) oxidation of glycine and glycylglycine: Kinetics and products. *Water Res.* **2010**, *44*, 927−935.
(11) Anquandah, G. A. K.; Sharma, V. K.; Knight, D. A.; Batchu, S. R.; Gardinali, P. R. Oxidation of trimethoprim by ferrate(VI): Kinetics, products, and antibacterial activity. *Environ. Sci. Technol.* **2011**, *45*, 10575−10581.
(12) Yang, B.; Ying, G.-G.; Zhang, L.-J.; Zhou, L.-J.; Liu, S.; Fang, Y.-X. Kinetics modeling and reaction mechanism of ferrate(VI) oxidation of benzotriazoles. *Water Res.* **2011**, *45*, 2261−2269.
(13) Zimmermann, S. G.; Schmukat, A.; Schulz, M.; Benner, J.; von Gunten, U.; Ternes, T. A. Kinetic and mechanistic investigations of the oxidation of tramadol by ferrate and ozone. *Environ. Sci. Technol.* **2012**, *46*, 876−884.
(14) Yang, B.; Ying, G.-G.; Zhao, J.-L.; Liu, S.; Zhou, L.-J.; Chen, F. Removal of selected endocrine disrupting chemicals (EDCs) and pharmaceuticals and personal care products (PPCPs) duirng ferrate-(VI) treatment of secondary wastewater effluents. *Water Res.* **2012**, *46*, 2194−2204.
(15) Prucek, R.; Tucek, J.; Kolarik, J.; Filip, J.; Marusak, Z.; Sharma, V. K.; Zboril, R. Ferrate(VI)-induced arsenite and arsenate removal by in situ structural incorporation into magnetic iron(III) oxide nanoparticles. *Environ. Sci. Technol.* **2013**, *47*, 3283−3292.
(16) Casbeer, E. M.; Sharma, V. K.; Zajickova, Z.; Dionysiou, D. D. Kinetics and mechanism of oxidation of tryptophan by ferrate(VI). *Environ. Sci. Technol.* **2013**, *47*, 4572−4580.
(17) Yang, B.; Ying, G. G. Oxidation of benzophenone-3 during water treatment with ferrate(VI). *Water Res.* **2013**, *47*, 2458−2466.
(18) Yang, X.; Guo, W.; Zhang, X.; Chen, F.; Ye, T.; Liu, W. Formation of disinfection by-products after pre-oxidation with chlorine dioxide or ferrate. *Water Res.* **2013**, *47*, 5856−5864.
(19) Sharma, V. K. Oxidation of inorganic contaminants by ferrates (VI, V, and IV)-kinetics and mechanisms: A review. *J. Environ. Manage.* **2011**, *92*, 1051−1073.
(20) Sharma, V. K. Ferrate(VI) and ferrate(V) oxidation of organic compounds: Kinetics and mechanism. *Coord. Chem. Rev.* **2013**, *257*, 495−510.
(21) Rush, J. D.; Zhao, Z.; Bielski, B. H. J. Reaction of ferrate(VI)/ferrate(V) with hydrogen peroxide and superoxide anion- a stopped-flow and premix pulse radiolysis study. *Free Radiat. Res.* **1996**, *24*, 187−198.
(22) Sharma, V. K.; Burnett, C. R.; Millero, F. J. Dissociation constants of the monoprotic ferrate(VI) ion in NaCl media. *Phys. Chem. Chem. Phys.* **2001**, *3*, 2059−2062.
(23) Rush, J. D.; Cyr, J. E.; Zhao, Z. W.; Bielski, B. H. J. The oxidation of phenol by ferrate(VI) and ferrate(V)-a pulse radiolysis and stopped-flow study. *Free Radiat. Res.* **1995**, *22*, 349−360.
(24) Johnson, M. D.; Hornstein, B. J. The kinetics and mechanism of the ferrate(VI) oxidation of hydroxylamines. *Inorg. Chem.* **2003**, *42*, 6923−6928.
(25) Goff, H.; Murmann, R. K. Studies on the mechanism of isotopic oxygen exchange and reduction of ferrate(VI) ion (FeO_4^{2-}). *J. Am. Chem. Soc.* **1971**, *93*, 6058−6065.
(26) Johnson, M. D.; Bernard, J. Kinetics and mechanism of the ferrate oxidation of sulfite and selenite in aqueous media. *Inorg. Chem.* **1992**, *31*, 5140−5142.
(27) Sharma, V. K. Oxidation of inorganic compounds by ferrate(VI) and ferrate(V): One-electron and two-electron transfer steps. *Environ. Sci. Technol.* **2010**, *44*, 5148−5152.
(28) Logager, T.; Holcman, J.; Sehested, K.; Pedersen, T. Oxidation of ferrous ions by ozone in acidic solutions. *Inorg. Chem.* **1992**, *31*, 3523−3529.
(29) Martire, D. O.; Caregnato, P.; Furlong, J.; Allegretti, P.; Gonzalez, M. C. Kinetic study of the reactions of oxoiron(IV) with aromatic substrates in aqueous solutions. *Int. J. Chem. Kinet.* **2002**, *34*, 488−494.
(30) Pestovsky, O.; Bakac, A. Reactivity of aqueous Fe(IV) in hydride and hydrogen atom transfer reactions. *J. Am. Chem. Soc.* **2004**, *126*, 13757−13764.
(31) Pestovsky, O.; Stoian, S.; Bominaar, E. L.; Shan, X.; Munck, E.; Que, L., Jr.; Bakac, A. Aqueous Fe^{IV}=O: Spectroscopic identification and oxo-group exchange. *Angew. Chem., Int. Ed.* **2005**, *44*, 6871−6874.
(32) Pestovsky, O.; Bakac, A. Aqueous ferryl(IV) ion: Kinetics of oxygen atom transfer to substrates and oxo exchange with solvent water. *Inorg. Chem.* **2006**, *45*, 814−820.
(33) Sharma, V. K.; O'Connor, D. B.; Cabelli, D. E. Sequential one-electron reduction of Fe(V) to Fe(III) by cyanide in alkaline medium. *J. Phys. Chem. B* **2001**, *105*, 11529−11532.
(34) Rush, J. D.; Bielski, B. H. J. Kinetics of ferrate(V) decay in aqeuous solution. *Inorg. Chem.* **1989**, *28*, 3947−3951.
(35) Rush, J. D.; Bielski, B. H. J. Decay of ferrate(V) in neutral and acidic solutions. A premix pulse radiolysis study. *Inorg. Chem.* **1994**, *33*, 5499−5502.
(36) Melton, J. D.; Bielski, B. H. J. Studies of the kinetic, spectral and chemical properties of Fe(IV) pyrophosphate by pulse radiolysis. *Radiat. Phys. Chem.* **1990**, *36*, 725−733.
(37) Lee, Y.; Yoon, J.; von Gunten, U. Spectrophotometric determination of ferrate (Fe(VI)) in water by ABTS. *Water Res.* **2005**, *39*, 1946−1953.
(38) Carr, J. D.; Kelter, P. B.; Tabatabai, A.; Splichal, D.; Erickson, J.; McLaughlin, C. W. Properties of ferrate(VI) in aqueous solution: An alternative oxidant in wastewater treatment. *Proc. Conf. Water Chlorinated Chem. Environ. Impact. Health Effects* **1985**, *5*, 1285−1298.
(39) Sarma, R.; Angeles-Boza, A. M.; Brinkley, D. W.; Roth, J. P. Studies of the di-iron(VI) intermediate in ferrate-dependent oxygen evolution from water. *J. Am. Chem. Soc.* **2012**, *134*, 15371−15386.
(40) Bielski, B. H. J.; Thomas, M. J. Studies of hypervalent iron in aqueous solutions. 1. Radiation-induced reductions of iron(VI) to iron(V) by CO_2^-. *J. Am. Chem. Soc.* **1987**, *109*, 7761−7764.
(41) Flyunt, R.; Leitzke, A.; Mark, G.; Mvula, E.; Reisz, E.; Schick, R.; von Sonntag, C. Determination of $^{\bullet}OH$, $O_2^{\bullet-}$, and hydroperoxide yields in ozone reactions in aqueous solution. *J. Phys. Chem.* **2003**, *107*, 7242−7253.
(42) Elovitz, M. S.; von Gunten, U. Hydroxyl radical/ozone ratios during ozonation processes. I. The R_{ct} concept. *Ozone Sci. Eng.* **1999**, *21*, 239−260.
(43) Voelker-Bartschat, B. M. *Iron Redox Cycling in Surface Waters: Effects of Humic Substances and Light*. Ph.D. Thesis; ETH Zürich: Zürich, 1994.
(44) Stookey, L. L. Ferrozine-A new spectrophotometric reagent for ion. *Anal. Chem.* **1970**, *42*, 779−781.
(45) Ianni, J. C. Kintecus Version 4.55. www.kintecus.com, 2012.
(46) Scott, S. L.; Chen, W. J.; Bakac, A.; Espenson, J. H. Spectroscopic parameters, electrode-potentials, acid ionization-constants, and electron-exchange rates of the 2,2′-azinobis(3-ethylbenzothiazoline-6-sulfonate) radicals and ions. *J. Phys. Chem.* **1993**, *97*, 6710−6714.
(47) Kamachi, T.; Kouno, T.; Yoshizawa, K. Participation of multioxidants in the pH dependence of the reactivity of ferrate(VI). *J. Org. Chem.* **2005**, *70*, 4380−4388.
(48) Sharma, V. K.; Bielski, B. H. J. Reactivity of ferrate(VI) and ferrate(V) with amino acids. *Inorg. Chem.* **1991**, *30*, 4306−4310.
(49) Johnson, M. D.; Sharma, K. D. Kinetics and mechanism of the reduction of ferrate by one-electron reductants. *Inorg. Chim. Acta* **1999**, *293*, 229−233.